The Journal of Immunology

Roles of Aluminum Hydroxide and Monophosphoryl Lipid A Adjuvants in Overcoming CD4$^+$ T Cell Deficiency To Induce Isotype-Switched IgG Antibody Responses and Protection by T-Dependent Influenza Vaccine

Eun-Ju Ko, Young-Tae Lee, Ki-Hye Kim, Youri Lee, Yu-Jin Jung, Min-Chul Kim, Yu-Na Lee, Taeuk Kang and Sang-Moo Kang

J Immunol 2017; 198:279-291; Prepublished online 23 November 2016;
doi: 10.4049/jimmunol.1600173
http://www.jimmunol.org/content/198/1/279

The Journal of Immunology is published twice each month by
The American Association of Immunologists, Inc.,
1451 Rockville Pike, Suite 650, Rockville, MD 20852

Print ISSN: 0022-1767 Online ISSN: 1550-6606.

Roles of Aluminum Hydroxide and Monophosphoryl Lipid A Adjuvants in Overcoming CD4$^+$ T Cell Deficiency To Induce Isotype-Switched IgG Antibody Responses and Protection by T-Dependent Influenza Vaccine

Eun-Ju Ko,* Young-Tae Lee,* Ki-Hye Kim,* Youri Lee,* Yu-Jin Jung,* Min-Chul Kim,*,† Yu-Na Lee,*,† Taeuk Kang,* and Sang-Moo Kang*

Vaccine adjuvant effects in the CD4-deficient condition largely remain unknown. We investigated the roles of combined monophosphoryl lipid A (MPL) and aluminum hydroxide (Alum) adjuvant (MPL+Alum) in inducing immunity after immunization of CD4 knockout (CD4KO) and wild-type (WT) mice with T-dependent influenza vaccine. MPL+Alum adjuvant mediated IgG isotype-switched Abs, IgG-secreting cell responses, and protection in CD4KO mice, which were comparable to those in WT mice. In contrast, Alum adjuvant effects were dependent on CD4$^+$ T cells. MPL+Alum adjuvant was effective in recruiting monocytes and neutrophils as well as in protecting macrophages from Alum-mediated cell loss at the injection site in CD4KO mice. MPL+Alum appeared to attenuate MPL-induced inflammatory responses in WT mice, likely improving the safety. Additional studies in CD4-depleted WT mice and MHC class II KO mice suggest that MHC class II$^+$ APCs contribute to providing alternative B cell help in the CD4-deficient condition in the context of MPL+Alum–adjuvanted vaccination. ***The Journal of Immunology*****, 2017, 198: 279–291.**

Successful vaccination is the most effective measure to prevent disease against future pathogens. In general, nonreplicating subunit vaccines are safer than live attenuated vaccines but typically require adjuvants for successful Ag-specific immune responses. Aluminum hydroxide (Alum) has a long history of usage as an adjuvant in human vaccines, and a gel suspension of Alum (Alhydrogel) is the common clinical formulation. Alum adjuvant effects have a bias toward promoting Th2 Ab responses and would not be highly effective against intracellular viral pathogens. Inactivated H5 influenza split vaccine (Emerflu) and formalin-inactivated human respiratory syncytial virus vaccine with the Alum adjuvant formulations are symbolic failures of vaccination in humans (1, 2). Adjuvant system 04 (AS04) contains Alum and monophosphoryl lipid A (MPL), a TLR4 agonist, was tested by GlaxoSmithKline, and AS04-adjuvanted vaccines were licensed for humans (3–5). AS04 is a component of the hepatitis B virus vaccine Fendrix and the human papillomavirus vaccine Cervarix. Fendrix is licensed in the European Union, and Cervarix is licensed in the United States, European Union, Australia, and other countries.

Most adjuvants are involved in activating components of the innate immune system, which result in the outcomes of increasing adaptive immune responses (6, 7). In general, B cells require CD4$^+$ T cell help to produce isotype-switched IgG Abs against protein Ags (8, 9). The production of influenza-specific Abs was highly impaired in thymectomized mice (10) and in T cell–deficient mice (11). These studies demonstrate that induction of isotype-switched IgG Abs to viral protein Ags is dependent on the help from CD4$^+$ T cells. Professional APCs such as dendritic cells (DCs) of the innate immune system are required to activate a certain type of T cells. The activation status of DCs and cytokine milieu are known to determine whether T cells differentiate into Th1, Th2, Th17, follicular Th, or regulatory T cells (12). Bacterial LPS is a TLR4 agonist and a natural endotoxin adjuvant and has significantly contributed to our understanding of how vaccine adjuvant works (7). TLR4 signaling activates the NF-κB pathway, eventually producing inflammatory cytokines (IL-6, TNF-α) (13). Also, induction of type 1 IFNs by LPS stimulates DCs to express costimulatory molecules (CD40, CD80, CD86). TLR-mediated activation of DCs is thought to be a major mechanism dictating the type of T cells recruited by presenting an Ag to specific T cells in lymphoid tissues, and leading to specific CD4$^+$ T cell clonal expansion and differentiation (14). Thus, it is thought that vaccine adjuvants educate certain CD4$^+$ T cells, subsequently orchestrating the quantity and quality of B cell responses via Ab isotype switching, as well as long-lived plasma and memory B cells.

In this study, we sought to determine whether the effects of combined MPL and Alum (MPL+Alum), MPL, and Alum adjuvants would require CD4$^+$ T cells in inducing IgG isotype-switched Abs and protection in the context of T-dependent influenza virus vaccine. MPL is an attenuated version of LPS. IgG isotype Abs and protective efficacy were determined in wild-type (WT) and CD4 knockout (CD4KO) mice after immunization with adjuvanted

*Center for Inflammation, Immunity and Infection, Institute for Biomedical Sciences, Georgia State University, Atlanta, GA 30303; and †Animal and Plant Quarantine Agency, Gimcheon 39660, Republic of Korea

Received for publication January 28, 2016. Accepted for publication October 24, 2016.

This work was supported by National Institutes of Health/National Institute of Allergy and Infectious Diseases Grants AI105170, AI119366, and AI093772 (all to S.-M.K.).

Address correspondence and reprint requests to Dr. Sang-Moo Kang, Center for Inflammation, Immunity and Infection, Institute for Biomedical Sciences, Georgia State University, 100 Piedmont Avenue, Atlanta, GA 30303. E-mail address: skang24@gsu.edu

Abbreviations used in this article: Alum, aluminum hydroxide; AS04, adjuvant system 04; ASC, Ab-secreting cell; BALF, bronchoalveolar lavage fluid; BM, bone marrow; BMDC, BM-derived DC; CD4KO, CD4 knockout; DC, dendritic cell; DN, double-negative; HAI, hemagglutination inhibition; KO, knockout; mDC, mature DC; MHCII, MHC class II; MPL, monophosphoryl lipid A; MPL+Alum, combined MPL and Alum; pDC, plasmacytoid DC; SpO_2, blood oxygen saturation; Vac, inactivated and detergent split virus; Vac+, vaccine plus; WT, wild-type.

www.jimmunol.org/cgi/doi/10.4049/jimmunol.1600173

T-dependent influenza virus vaccine. In vitro and in vivo mechanistic studies were carried out to gain further insight into the action mechanisms of MPL+Alum adjuvant. This study reveals a new paradigm of CD4-independent MPL+Alum combination adjuvant mechanism as well as possible roles of Alum and MPL in combination MPL+Alum adjuvant effects.

Materials and Methods

Animals and reagents

Female and male 6- to 8-wk-old C57BL/6, CD4KO (B6.129S6-*Cd4*^{tm1Mak}/J), and MHC class II (MHCII) KO (I-A$\beta^{-/-}$) mice were purchased from The Jackson Laboratory and maintained in the animal facility at Georgia State University. All mouse experiments followed the approved Georgia State University Institutional Animal Care and Use Committee protocol (A14025). Commercial human monomeric influenza vaccine (inactivated and detergent split virus [Vac]), derived from the 2009 pandemic strain of A/California/07/2009 H1N1 virus, was provided by Green Cross (South Korea), a World Health Organization–approved vaccine manufacturing company. MPL and Alum were purchased from Sigma-Aldrich. MTT was obtained from Sigma-Aldrich for cell death analysis.

Immunization and infection

Mice were immunized i.m. with influenza vaccine alone or adjuvanted with 5 μg of MPL, 50 μg of Alum, or 5 μg of MPL plus 50 μg of Alum (MPL+Alum). For Ag adsorption of Alum or MPL+Alum adjuvant, influenza vaccine was incubated with adjuvant at 37˚C for 30 min before immunization. The immunizations were performed twice (prime and boost) in WT, CD4KO, and MHCII KO mice with an interval of 4 wk, and immune sera were collected at 3 wk after each immunization (see Fig. 1A). To determine MPL+Alum adjuvant effects in primed mice, WT mice were primed with split influenza vaccine only, and then boosted with vaccine only or vaccine plus (Vac+)MPL+Alum. For CD4$^+$ T cell acute depletion in WT mice, naive WT mice were injected with anti-mouse CD4 mAb (200 μg/mouse, clone GK1.5) i.p. 2 d before each prime and boost immunization. To maintain CD4 depletion status, the mice were injected with CD4-depleting Abs every 7 d. At 20 wk after boost, naive and immunized mice were challenged with 17-fold the LD_{50} of A/California/04/2009 (H1N1) virus. The challenged mice were monitored to determine survival rates and body weight changes for 14 d. Kaplan–Meier analysis and log rank were applied for the survival graphs. Additional sets of challenged mice were sacrificed at day 5 after infection to determine protective efficacy. After sacrifice, bronchoalveolar lavages fluid (BALF), lung, bone marrow (BM), and spleens were harvested for further analysis.

ELISAs

For ELISA of serum IgG and IgG isotypes, the serially diluted sera were applied to the ELISA plates (Costar) coated with inactivated A/California/04/2009 H1N1 virus as previously described (15). Levels of IgG and IgG isotypes were determined by using anti-mouse IgG, IgG1, or IgG2c HRP conjugates as secondary Abs and tetramethylbenzidine as a substrate (16). Cytokines and chemokines in BALF, lung extract, peritoneal exudates, sera, and cell culture supernatants were measured by using ELISA kits from eBioscience and R&D Systems.

Hemagglutination inhibition assay

Sera and receptor destroying enzyme were mixed at a 3:1 ratio and incubated in 37˚C for 16 h, and then followed by heat treatment at 56˚C for 30 min. The sera were serially diluted (final volume of 25 μl) and incubated with 8 hemagglutination units of A/California/04/2009 H1N1 virus (final volume of 25 μl) in V-bottom plates for 30 min. Chicken RBCs (50 μl, 0.5%) were added to the plates and hemagglutination inhibition (HAI) titers were determined after 40 min.

Protective assay of immune sera

Naive and immune sera were incubated at 56˚C for 30 min for complement inactivation and mixed with a lethal dose of A/California/04/2009 (H1N1) virus. After 30 min, the mixture of sera (25 μl of 2-fold serial diluted sera) and virus was used to infect naive WT mice (n = 5) intranasally. Body weight changes and survival rates of the infected mice were daily monitored for 14 d.

Lung virus titration

Lung samples were harvested from the immunized mice at day 5 postinfection. The lung extracts were diluted and injected into 9- to 10-d-old embryonated chicken eggs. The allantoic fluids were collected after 3 d of incubation and used to perform hemagglutination activity assays to determine 50% egg infective dose.

Lung histology

Mouse lung tissue samples were harvested at 5 d after virus infection and treated with 10% of neutral formalin for fixation. The fixed lung tissues were sectioned and stained with H&E as described (17, 18). Images were acquired by a microscope (Zeiss Axiovert 100) at ×100 magnification and an attached camera (Canon 30D).

Intraperitoneal injection

WT and CD4KO mice were injected with 200 μl of PBS, MPL (5 μg) + Alum (50 μg), MPL (5 μg), or Alum (50 μg) i.p. Sera were collected at 1.5, 6, and 24 h postinjection for detection of cytokines and chemokines. Peritoneal exudates were harvested at 24 h postinjection by PBS flushing. Peritoneal cells were used to determine phenotypes and cellularity of infiltrating cells by flow cytometry, and peritoneal exudates were used for detection of cytokines and chemokines.

In vitro cell cultures

BM-derived DCs (BMDCs) were generated from BM cells with mouse GM-CSF as described (19). The cells were treated with MPL (5 μg) + Alum (50 μg), MPL (5 μg), or Alum (50 μg) to determine proinflammatory cytokine production, DC activation marker expression, and cell death by adjuvants. For measuring in vitro IgG production by adjuvant-stimulated BMDCs, Vac (3 μg) + MPL (5 μg) + Alum (50 μg) combination was used to pretreat BMDCs for 2 d for preparation of mature DCs (mDCs). Spleen cells from naive CD4KO mice were cultured with MPL+Alum, mDCs, or mDCs plus mDC culture supernatant for 7 d. IgG levels in culture supernatants were determined by ELISA. To determine proliferated double-negative (DN) T cells, spleen cells were harvested from Vac+MPL+Alum–immunized CD4KO mice and stained with CFSE. The CFSE-labeled cells were cocultured with immature DCs, mDCs, or mDC plus anti-mouse MHCII mAbs (1 μg/ml, clone M5/114.15.2) for 5 d. For Ag-specific DN T cell proliferation, OVA (1 μg/ml)-, inactivated A/Philippine H3N2 (3 μg/ml)–, or inactivated A/California H1N1 vaccine strain (3 μg/ml)–treated BMDCs were cultured with CFSE-labeled cells for 5 d. The percentages of DN T cell proliferation were measured by flow cytometry.

Flow cytometry

Cells harvested after i.p. injection were stained with fluorescence-labeled anti-mouse F4/80, Ly6c, CD11b, CD11c, Siglec-F, CD103, B220, CD3, CD4, CD8, and CD49b Abs after blocking Fc receptor (anti-mouse CD16/32) to determine cellular phenotypes recruited by adjuvant injection. Adjuvant-treated BMDCs were harvested and stained with fluorescence-labeled anti-mouse CD40, CD80, CD86, and MHCII Abs after blocking Fc receptors (anti-mouse CD16/32). The stained cells were acquired by BD LSRFortessa (BD Biosciences, Mountain View, CA) and analyzed by FlowJo (Tree Star, Ashland, OR).

Statistical analysis

Experimental data were presented as means ± SEM. The statistical significance was determined by one-way ANOVA followed by a Tukey multiple comparison test or by two-way ANOVA followed by a Bonferroni posttest. A p value <0.05 was considered significant. We analyzed all data with Prism software (GraphPad Software, San Diego, CA).

Results

MPL+Alum– and MPL-adjuvanted influenza vaccines induce isotype-switched IgG Abs in CD4KO mice

To determine whether adjuvanted vaccination would overcome a defect in CD4$^+$ T cells for inducing isotype-switched IgG Abs, WT and CD4KO mice were i.m. immunized with influenza vaccine or in the presence of MPL+Alum, MPL, or Alum adjuvant (n = 10). At 3 wk after prime, the influenza vaccine (WT-Vac) and Alum (WT-Alum) groups of WT mice showed low levels of virus-specific IgG Abs (Fig. 1B). CD4KO mice with vaccine (KO-Vac)

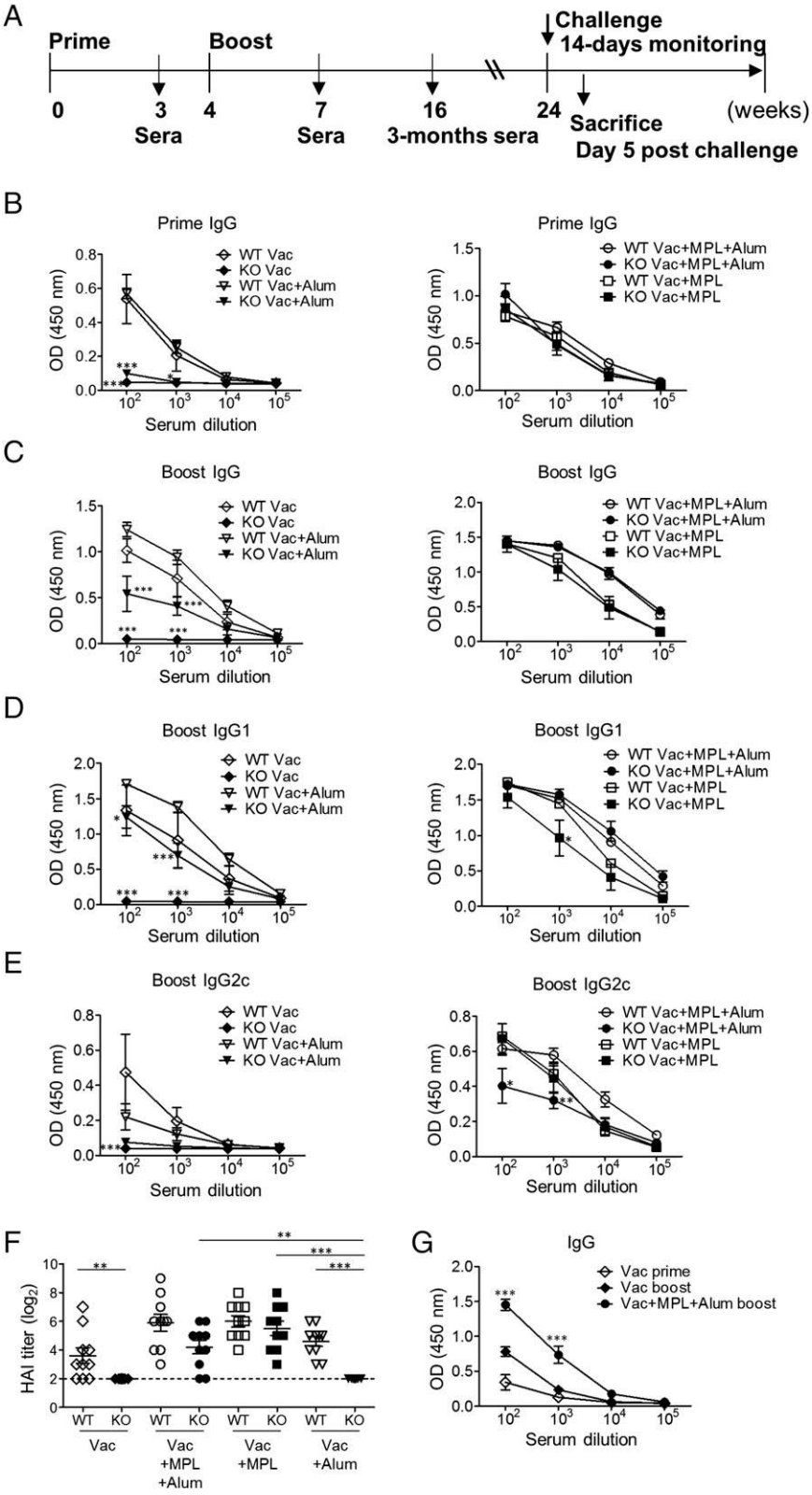

FIGURE 1. MPL+Alum–adjuvanted vaccination induces isotype-switched IgG Abs regardless of $CD4^+$ T cells. (**A**) Schematic diagram of vaccination schedule and assessment of protective efficacy. KO, CD4KO mice; Vac, inactivated influenza virus split vaccine (Vac) only immunized group; Vac+Alum, influenza split vaccine plus Alum-immunized group; Vac+MPL; influenza split vaccine plus MPL-immunized group; Vac+MPL+Alum, influenza split vaccine plus MPL plus Alum-immunized group; WT, C57BL/6 WT mice. (**B**) Prime IgG Ab levels of immunized WT and CD4KO mice. (**C**) Boost IgG Ab levels of immunized WT and CD4KO mice. (**D**) Boost IgG1 isotype Ab levels of immunized WT and CD4KO mice. (**E**) Boost IgG2c isotype Ab levels of WT and CD4KO mice. Immune sera were collected 3 wk after prime and boost immunization from WT and CD4KO mice ($n = 10$ per group). Inactivated virus–specific IgG Ab levels were determined by ELISA and are shown as mean ± SEM of OD. Statistical significances were calculated by two-way ANOVA and Bonferroni posttests. $*p < 0.05$, $**p < 0.01$, $***p < 0.001$ compared between each corresponding WT and CD4KO groups. (**F**) HAI titers were determined from immune sera of vaccine with and without MPL+Alum, MPL, or Alum adjuvant–immunized WT and CD4KO mice. The detection limit of HAI titer was 2. Statistical significance was calculated by one-way ANOVA and followed by a Tukey multiple comparison test. $**p < 0.01$, $***p < 0.001$ as indicated among the groups. (**G**) IgG Ab levels of WT mice. All mice were primed with vaccine only, and then vaccine-primed mice were boosted with vaccine only or Vac+MPL+Alum. Statistical significance was calculated by a two-way ANOVA and a Bonferroni posttest. $***p < 0.001$ compared with Vac boost group.

only or Alum-adjuvanted (KO-Alum) vaccination did not induce virus-specific IgG Abs after prime (Fig. 1B), suggesting that vaccine is a T-dependent Ag and that Alum adjuvant effects are dependent on $CD4^+$ T cells. Surprisingly, the MPL+Alum and MPL adjuvant groups induced IgG Abs in CD4KO (KO-Vac+MPL+Alum, KO-Vac+MPL) mice at high levels comparable to the corresponding WT groups (WT-Vac+MPL+Alum, WT-Vac+MPL) after prime immunization (Fig. 1B). Therefore, MPL+Alum combination and MPL adjuvants can overcome a defect of $CD4^+$ T cells in priming IgG Abs to T-dependent influenza vaccine in CD4KO mice.

When we determined IgG Abs in boost-vaccinated WT and CD4KO mice (Fig. 1C), the vaccine alone KO group did not induce IgG Abs whereas the WT-Vac group showed substantial

levels of IgG with dominant IgG1 (Th2 type) isotype (Fig. 1D, 1E). Also, the KO-Vac+Alum group showed a significantly lower level of IgG and IgG1 Abs compared with those in WT-Alum mice (Fig. 1C, 1D), indicating that CD4$^+$ T cells are required for Alum adjuvant effects. The KO-MPL+Alum group exhibited high levels of IgG and IgG1 isotype Abs, which are comparable to those in WT-MPL+Alum mice and higher than the KO-MPL group (Fig. 1C, 1D). The KO-Vac+MPL group displayed boost IgG Abs comparable to those in WT mice (Fig. 1C) but a trend of lower levels of IgG1 Abs compared with those in WT mice (Fig. 1D). Induction of low IgG2c (Th1 type) levels was observed in the WT-Vac and WT-Vac+Alum groups but not the corresponding KO groups (Fig. 1E). The KO-Vac+MPL+Alum group induced IgG2c Abs at substantial but lower levels compared with those in the corresponding WT mice (Fig. 1E). The KO-Vac+MPL group was effective in inducing IgG2c isotype Abs to an equivalent level as observed in the corresponding WT mice (Fig. 1E). We observed that IgG Ab levels in KO-MPL and particularly in KO-MPL+Alum mice kept increasing when determined at 3 mo after boost vaccination (Table I), which were still maintained for >9 mo (data not shown). Importantly, note that MPL+Alum– and MPL-adjuvanted vaccination of CD4KO mice induced IgG Abs to comparable levels in the corresponding WT mouse vaccination.

Serum HAI titers are used as a measure of functional Abs predicting the efficacy of protection against influenza virus. The WT-Vac and WT-Alum groups showed a trend of lower levels of HAI titers compared with those in the WT-MPL+Alum and WT-MPL groups. Vaccine only and Vac+Alum–immunized CD4KO mice did not induce detectable levels of HAI titers (Fig. 1F). In contrast, the KO-MPL+Alum and KO-MPL groups showed high levels of HAI titers similar to those in WT-MPL+Alum and WT-MPL immune mice, and there were no statistical significances in the corresponding WT and KO groups (Fig. 1F). Thus, MPL+Alum or MPL adjuvant in influenza vaccination can induce protective Abs in CD4KO mice at comparable levels as observed in corresponding WT-adjuvant immune mice.

To determine adjuvant effects of MPL+Alum in primed mice, we primed WT mice with vaccine only and then boosted the mice with vaccine only or Vac+MPL+Alum. The boosted mice with MPL+Alum showed significantly higher levels of IgG Ab responses (Fig. 1G, Vac+MPL+Alum boost; 13.6 ± 2.47 μg/ml) compared with the vaccine only primed and boosted mice (Fig. 1G, Vac boost; 3.71 ± 0.48 μg/ml).

MPL+Alum- or MPL-adjuvanted vaccination of CD4KO mice induces protection against influenza virus

To determine adjuvant effects on improving the efficacy of protection, naive and immunized WT and CD4KO mice were intranasally challenged with a lethal dose of A/California/04/2009 (H1N1) virus after 5 mo of vaccination (Fig. 2). Both CD4KO and WT naive mice all died by days 8 and 10 postinfection, respectively. The WT-Vac group showed severe weight loss of ~18%, resulting in 60% of survival rates, whereas the KO-Vac group did not show any protection, similar to naive infection mice (Fig. 2A, 2B). The WT-Alum group displayed moderate weight loss of 9–10 and 100% survival rates. In contrast, KO-Alum immune mice were very sick, as indicated by 18% weight loss at a peak point, and thus resulted in only 40% survival rates. Both the WT-MPL+Alum and WT-MPL groups showed 100% protection without weight loss (Fig. 2A). Also, KO-MPL+Alum and KO-MPL mice were similarly well protected against the same lethal dose challenge as used in WT mice, although a transient weight loss was observed in these KO mice at 6–9 d after challenge, probably due to the lack of CD4$^+$ T cells (Fig. 2A, 2B).

At day 5 after challenge, lung viral titers were measured to determine the efficacy of clearing lung viral loads (Fig. 2C). The naive, vaccine only, and Vac+Alum groups showed high levels of viral loads in WT and particularly in CD4KO mice, which are consistent with low or no HAI titers, severe weight loss, and low survival rates in these groups. MPL+Alum and MPL adjuvant in the vaccination led to low lung viral titers, and there were no statistical differences between WT and CD4KO mice, although the MPL+Alum group showed a trend of increasing viral titers in CD4KO mice.

To further determine the protective roles of immune sera from CD4KO mice, we infected naive mice with a mixture of a lethal dose of A/California/04/2009 (H1N1) virus and immune sera or naive sera. All naive mice that were infected with virus plus naive or vaccine only sera died at day 8 or 9 postinfection (Fig. 2D). The naive mice infected with virus- and Alum-adjuvanted vaccination sera showed 10% body weight loss, but naive mice that received MPL+Alum– or MPL-adjuvanted immune sera did not show any weight loss (Fig. 2D). Overall, these results provide evidence that MPL+Alum– or MPL-adjuvanted vaccination induces protective immunity against lethal infection in CD4KO mice at a comparable level to that observed in WT mice.

Table I. Kinetics of IgG levels in immunized mice

	Immunization	3 Wk after Prime	3 Wk after Boost	3 Mo after Boost
C57BL/6 WT	Vac	3.11 ± 1.82	13.10 ± 3.94	12.55 ± 2.46
	Vac+MPL+Alum	12.26 ± 1.16	26.44 ± 0.55	20.46 ± 3.50
	Vac+MPL	10.44 ± 0.86	22.83 ± 1.19	21.61 ± 1.52
	Vac+Alum	4.06 ± 0.69	17.73 ± 1.55	17.89 ± 1.53
CD4KO	Vac	n.d.	n.d.[b]	0.22 ± 0.09[a]
	Vac+MPL+Alum	8.85 ± 0.86	26.00 ± 1.15	28.88 ± 3.23
	Vac+MPL	8.76 ± 2.26	19.63 ± 3.09	24.70 ± 5.34
	Vac+Alum	n.d.	7.13 ± 1.96[a]	2.45 ± 0.9644[b]
CD4-depleted C57BL/6 WT	Vac+MPL+Alum	0.40 ± 0.44[b,d]	2.66 ± 1.1544[b,d]	ND
	Vac+MPL	2.15 ± 1.3144[b,c]	6.83 ± 2.2944[b,d]	ND
MHCII KO	Vac+MPL+Alum	0.06 ± 0.0644[b,d]	0.82 ± 0.3044[b,d]	ND
	Vac+MPL	n.d.	0.61 ± 0.1744[b,d]	ND

Immune sera were collected and ELISA was performed to determine Ag-specific IgG levels. Data are shown as mean concentrations (μg/ml) ± SEM.
Statistical analysis was performed by one-way ANOVA and a Tukey multiple comparison test.
[a] $p < 0.01$, [b] $p < 0.001$ compared with the corresponding C57BL/6 WT IgG levels of each time point.
[c] $p < 0.01$, [d] $p < 0.001$ compared with the corresponding CD4KO mice IgG levels of each time point.
n.d., not detected.

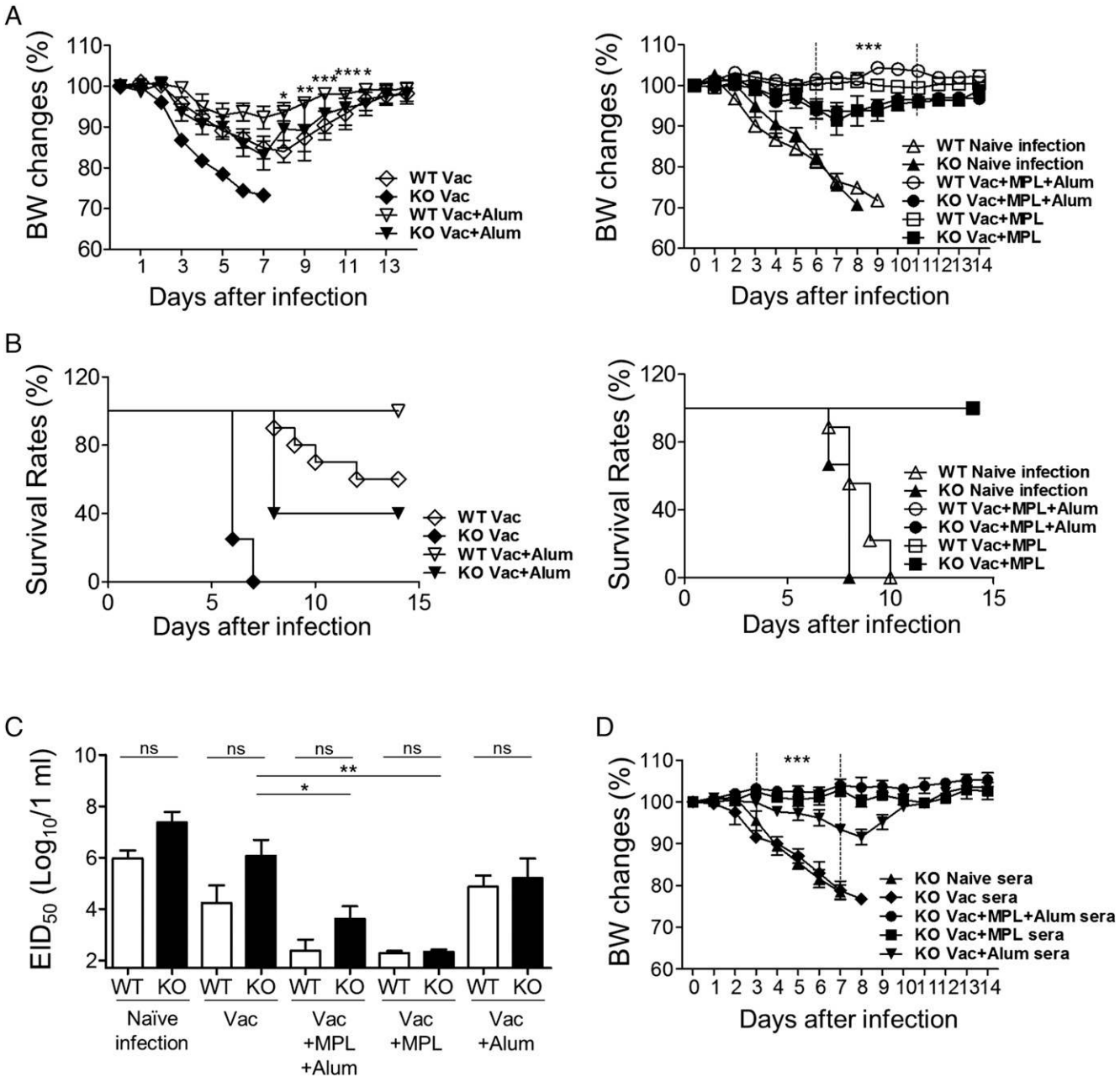

FIGURE 2. Protective efficacy of MPL+Alum or MPL-adjuvanted split vaccination against influenza virus in WT and CD4KO mice. (**A**) Body weight changes. (**B**) Survival rates. Immune mice ($n = 10$ per group) were challenged with a lethal dose of A/California/04/2009 virus 5 mo after boost immunization. Statistical significance was calculated by two-way ANOVA and followed by a Bonferroni posttest. $*p < 0.05$, $**p < 0.01$, $***p < 0.001$ compared with corresponding KO groups. (**C**) Lung virus titers. Lung viral titers were determined at day 5 postinfection by a 50% egg infective dose (EID_{50}). Data ($n = 10$) are shown as mean ± SEM. The detection limit of EID_{50} was 1.7. (**D**) Protective roles of immune sera. Naive and immune sera were incubated at 56°C for 30 min for complement inactivation and mixed with a lethal dose of A/California/04/2009 (H1N1) virus. After 30 min, the mixture of sera (25 μl containing a range of 0–24 HAI titers) and virus was used to infect naive WT mice ($n = 5$) intranasally. Body weight changes of the infected mice were daily monitored for 14 d. Statistical significance was calculated by one-way ANOVA and followed by a Tukey multiple comparison test or by two-way ANOVA and followed by a Bonferroni posttest. $*p < 0.05$, $**p < 0.01$, $***p < 0.001$ compared with vaccine only group or as indicated among the groups. ns, not significant.

MPL+Alum–adjuvanted influenza vaccination prevents lung disease due to viral infection of CD4KO mice

Influenza virus can cause severe lung inflammation, leading to pneumonia and high mortality. To better assess the protective effects of adjuvant vaccination on alleviating disease symptoms, blood oxygen saturation (SpO_2) levels were measured in live animals at day 4 after influenza virus infection by using oximetry (Fig. 3A). In both WT and CD4KO mice, the naive infection and vaccine only groups exhibited significantly lower SpO_2 levels of ~90% (Fig. 3A) compared with uninfected control mice. Low SpO_2 levels would indicate a severe breathing disorder caused by blocking the airways due to respiratory virus infection. In contrast, MPL+Alum–adjuvanted vaccination resulted in maintaining normal SpO_2 levels >98% in both WT and CD4KO mice.

Upon lethal influenza virus challenge, highest levels of inflammatory IL-6 and TNF-α cytokines were observed in WT-naive mice (Fig. 3B, 3C). Also, substantially high levels of IL-6 and TNF-α were detected in BALF from WT-naive, KO-naive, WT-Vac, KO-Vac, and KO-Alum mice at day 5 after challenge. In contrast, IL-6 and TNF-α cytokines were undetected or detected at low

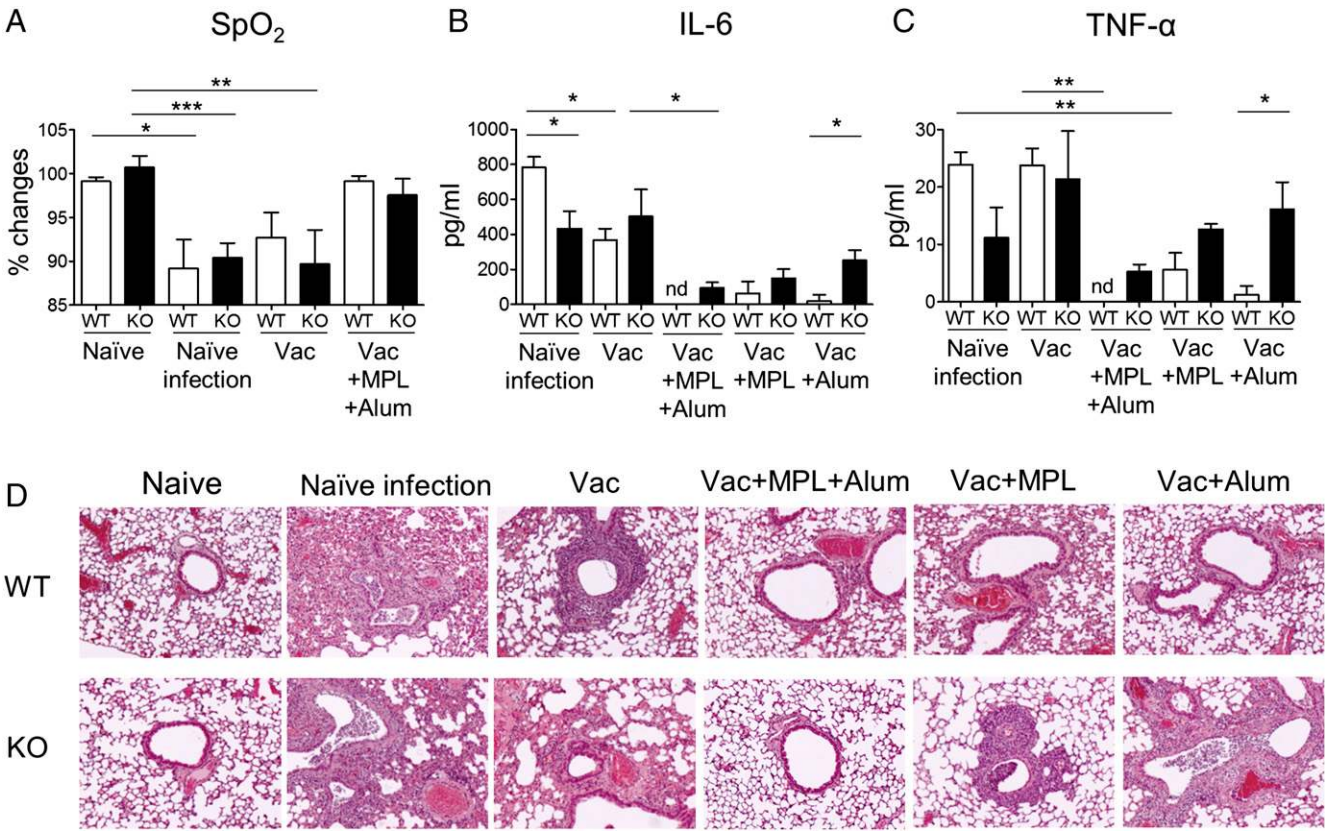

FIGURE 3. MPL+Alum–adjuvanted vaccination of CD4KO mice prevents lung inflammation after virus challenge. Immune mice (n = 10 per group) were challenged with a lethal dose of A/California/04/2009 virus. (**A**) At days 0 and 4 after virus infection, the SpO_2 values were measured by using oximetry. The changes of day 4 compared with those of day 0 are shown as percentages. (**B** and **C**) BALF samples were collected (n = 5 mice per group) at 5 d after a lethal dose of A/California/04/2009 H1N1 influenza virus infection and used to determine cytokine IL-6 (B) and TNF-α (C) levels. (**D**) Lung histopathology. Lung tissues from the infected mice (n = 5 mice per group) at day 5 after challenge were stained with H&E. Statistical significance was calculated by one-way ANOVA and a Tukey multiple comparison test. *$p < 0.05$, **$p < 0.01$, ***$p < 0.001$ as indicated among the groups. KO, CD4KO mice; nd, not detected; WT, C57BL/6 WT mice.

levels in BALF of WT-MPL+Alum and KO-MPL+Alum mice (Fig. 3B, 3C). KO-MPL mice displayed IL-6 and TNF-α cytokines in BALF at moderate levels (Fig. 3B, 3C). Thus, these results suggest that MPL+Alum–adjuvanted vaccination prevents the induction of proinflammatory cytokines even in CD4KO mice.

As for further evidence of lung inflammation, examination of lung histology showed that severe immune cell infiltration around the airways, alveolar septa, and interstitial spaces as well as narrowing or collapsing airways were observed in WT and CD4KO naive mice at day 5 postinfection (Fig. 3D), which are consistent with low SpO_2 levels. Significant lung histopathology was displayed in the WT-Vac, KO-Vac, and KO-Alum groups (Fig. 3D). Low to moderate histopathology, including thickening in the airway endothelial layers, was revealed in the WT-Alum, WT-MPL, and KO-MPL groups (Fig. 3D). Both WT-MPL+Alum and KO-MPL+Alum mice did not exhibit an overt sign of lung histopathology, indicating protection from lung inflammation due to influenza viral infection (Fig. 3D).

MPL+Alum–adjuvanted influenza vaccination induces Ab-secreting cell responses in WT and CD4KO mice

A goal of vaccination is to induce long-lived Ab-secreting cell (ASC) responses. Vaccinated mice were challenged after 5 mo of vaccination, and then BM and spleen cells were harvested at day 5 after challenge for analysis of IgG Abs secreted from ASCs in in vitro culture supernatants using ELISA (Fig. 4) as described (20). WT-Vac and WT-Alum mice showed only low levels of vaccine-specific IgG Ab production in BM cell cultures (Fig. 4A). BM cells from WT-MPL mice showed moderate levels of in vitro IgG Ab secretion whereas WT-MPL+Alum immune mouse BM cells produced significantly higher levels of IgG Abs after 1 d in vitro culture (Fig. 4A). As a measure of memory B cells, spleen cells were cultured for 5 d in the presence of inactivated virus (A/California/04/2009 H1N1). Spleen cells from WT-Alum mice produced low levels of IgG Abs. In contrast, WT-MPL+Alum groups of mice induced high levels of IgG Ab production in spleen cells (Fig. 4B).

$CD4^+$ T cells are required to induce long-lived isotype-switched IgG ASCs in BM after viral infection (21, 22). We determined whether certain adjuvants could mediate the in vitro production of IgG Abs in BM and spleen cells from CD4KO mice after 5 mo of vaccination at day 5 after challenge (Fig. 4). KO-Vac mice did not show in vitro IgG Ab production in BM and spleen cells. The KO-MPL+Alum and MPL groups showed high levels of in vitro IgG Ab production in BM cells, which are comparable to those in corresponding WT mice after 1 d in vitro culture (Fig. 4). MPL+Alum adjuvant was more effective in in vitro IgG protection in 5-d culture of CD4KO spleen cells compared with MPL. Consistent with in vivo IgG responses, MPL+Alum adjuvant may effectively mediate the generation of long-lived IgG ASCs in CD4KO mice comparable to those in WT mice.

Adjuvant effects on IgG Abs in CD4-depleted WT and MHCII KO mice support a role of MHCII-expressing cells in the alternative B cell help

CD4KO mice might have developed compensatory immune components contributing to the alternative B cell help. To test this possibility, $CD4^+$ T cells in WT mice were acutely depleted up to

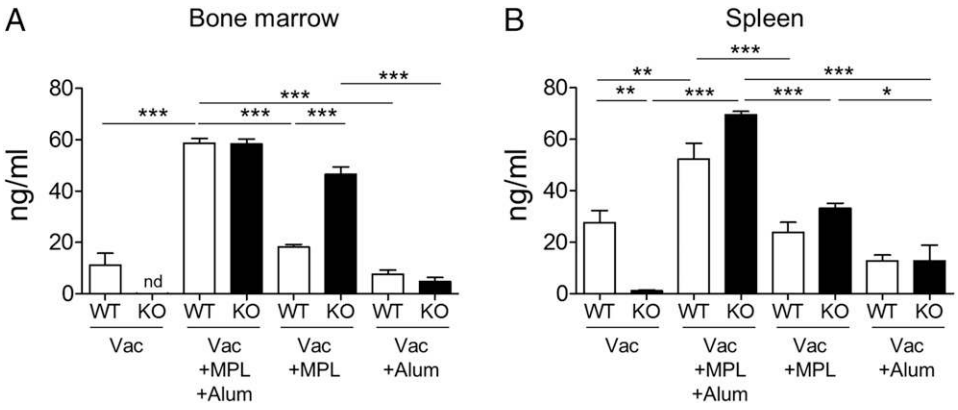

FIGURE 4. In vitro ASC responses in BM and spleens. (**A**) IgG production from BM cells of immunized WT and CD4KO mice. (**B**) IgG production of spleen cells of immunized WT and CD4KO mice. BM and spleen cells were harvested on day 5 postinfection after 5 mo of vaccination ($n = 5$). BM cells of WT and CD4KO mice were cultured for 1 d, and spleen cells of WT mice and CD4KO mice were cultured for 5 d in the presence of inactivated virus Ags. IgG levels were detected by ELISA. Statistical significance was calculated by one-way ANOVA and a Tukey multiple comparison test. $*p < 0.05$, $**p < 0.01$, $***p < 0.001$ as indicated among the groups. KO, CD4KO mice; WT, C57BL/6 WT mice.

>99% by CD4-depleting Ab treatment before and during adjuvanted prime and boost vaccination (Fig. 5A). Approximately 3-fold lower levels of IgG (mostly IgG1 isotype) Ab responses were induced in acute CD4-depleted WT mice with MPL-adjuvanted vaccination compared with those in CD4KO mice with the same adjuvanted vaccination (Fig. 5B, Table I). Also, acute CD4-depleted WT mice with MPL-adjuvanted vaccination displayed weight loss of ~8–12% (Fig. 5C), which is lower protective efficacy than that in CD4KO mice (Fig. 2A). CD4-depleted WT mice with MPL+Alum–adjuvanted vaccination showed 10-fold lower levels of IgG Abs compared with those in CD4KO mice (Table I). MHCII KO mice deficient in $CD4^+$ T cells in addition to a genetic defect in MHCII expression (16, 23) were used for adjuvanted influenza vaccination. The levels of IgG Abs in MHCII KO mice with MPL- or MPL+Alum–adjuvanted influenza vaccination were significantly lower by 32-fold compared with those in CD4KO mice (Table I). These experimental data suggest that compensatory immune components, particularly MHCII-expressing APCs, developed in CD4KO mice contribute to the

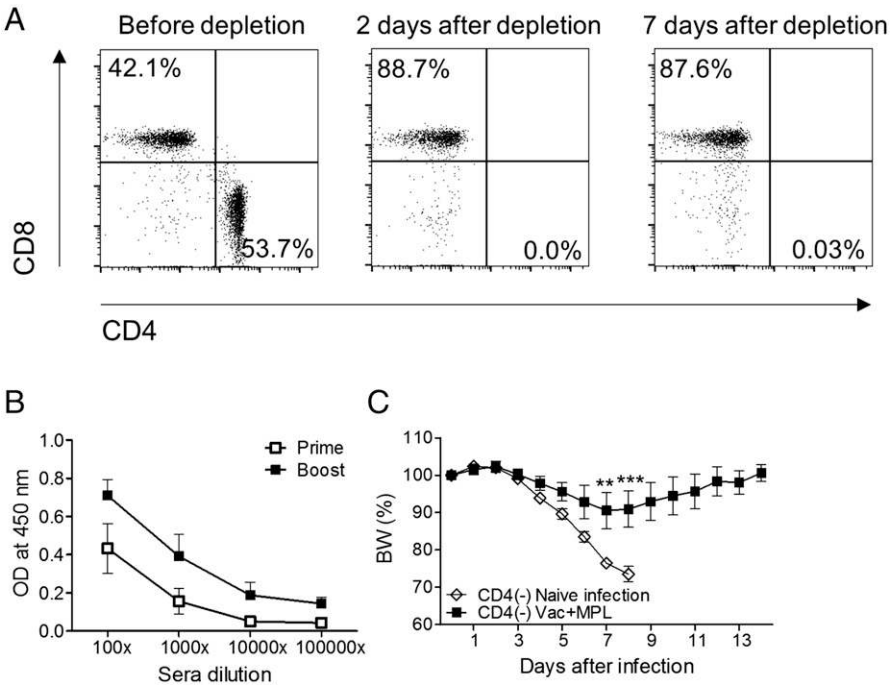

FIGURE 5. Ab production and protective efficacy of MPL-adjuvanted vaccination against influenza virus in CD4-depleted C57BL/6 WT mice. (**A**) C57BL/6 WT mice were injected with anti-CD4 mAb (200 μg/mouse, clone GK1.5) to deplete $CD4^+$ T cells. Blood cells from CD4-depleting Ab–treated mice were used to determine the efficacy of CD4 depletion. CD4 and CD8 marker profiles are shown from $CD3^+$-gated T cells. (**B**) Virus-specific Ab levels of immunized CD4-depleted mice after prime and boost immunization. CD4-depleted WT mice were immunized i.m. with Vac+MPL. To maintain CD4 depletion status, the mice were injected with CD4-depleting Abs every 7 d. Immune sera ($n = 5$ per group) were collected 2 wk after each immunization. Inactivated virus-specific Ab levels were determined by ELISA and are shown as mean ± SEM of OD. (**C**) Body weight changes of the CD4-depleted mice after lethal virus infection. Naive and the immunized CD4-depleted mice were challenged with a lethal dose of A/California/07/2009 (H1N1) virus intranasally. Body weight changes of the infected mice were daily monitored for 14 d. Statistical significance was calculated by two-way ANOVA and followed by a Bonferroni posttest. $**p < 0.01$, $***p < 0.001$ compared with naive infection group.

generation of isotype-switched IgG Abs, probably by providing an alternative form of T cell help.

MPL+Alum attenuates MPL-induced serum inflammatory cytokines and chemokines in WT mice

To determine adjuvant effects on innate responses in CD4KO mice, we injected adjuvants (MPL+Alum, MPL, Alum) i.p. to WT and CD4KO mice. Sera were taken at 1.5, 6, and 24 h after the injection and then the mice were sacrificed to collect peritoneal exudates. Cytokines and chemokines in peritoneal exudates and sera were determined by ELISA. MPL injection of WT mice acutely induced extreme high levels of proinflammatory cytokines (IL-6, TNF-α) and MCP-1 chemokine within 1.5 h systemically in blood, which were rapidly reduced within 6 h (Fig. 6A). In contrast, MPL +Alum did not acutely raise inflammatory cytokines and MCP-1 chemokine but induced a low level of TNF-α and MCP-1 at 6 h postinjection in sera of WT mice (Fig. 6A). Alum injection did not induce cytokines or chemokines. Therefore, these results suggest that Alum in the combination MPL+Alum adjuvant plays a role of attenuating acute inflammation due to MPL injection in WT mice.

A different pattern was observed after adjuvant injection in CD4KO mice (Fig. 6B). Serum IL-6 and TNF-α cytokines were induced to a moderate and low level, respectively, at 1.5 h and then lowered to a basal level within 6 h after MPL+Alum or MPL injection of CD4KO mice (Fig. 6B). MPL or MPL+Alum injection induced a high level of serum MCP-1 in CD4KO mice. These results indicate that MPL+Alum may have an effect on acutely inducing cytokines and MCP-1 chemokine in CD4KO mice, which is different from WT mice.

In contrast to acute cytokine levels in blood, we observed a different profile of cytokines and chemokines at the injection site after 24 h (Fig. 6C). MPL injection of WT or CD4KO mice induced low levels of chemokines (MCP-1, RANTES) in the peritoneal cavity after 24 h (Fig. 6C). Interestingly, MPL+Alum injection of CD4KO mice induced moderate levels of IL-6, TNF-α, MCP-1, and RANTES in the peritoneal cavity after 24 h, which are higher than those in MPL+Alum i.p. injection of WT mice (Fig. 6C).

MPL+Alum recruits a distinct pattern of innate immune cells at the injection site in CD4KO mice

Immune cell types and cellularity at the injection site might provide insight into mechanisms of adjuvant effects in CD4KO mice. We analyzed cell types recruited in the peritoneal cavity at 24 h after i.p. injection of mice with adjuvants. Naive WT mice maintain high cellularity of macrophages in the peritoneal cavity (Fig. 7A, 7B). Interestingly, Alum injection of WT mice resulted in almost complete depletion of macrophages (Fig. 7A, 7B) and lower cellularity of plasmacytoid DCs (pDCs; 17%, Fig. 7I) and CD11b^{low}

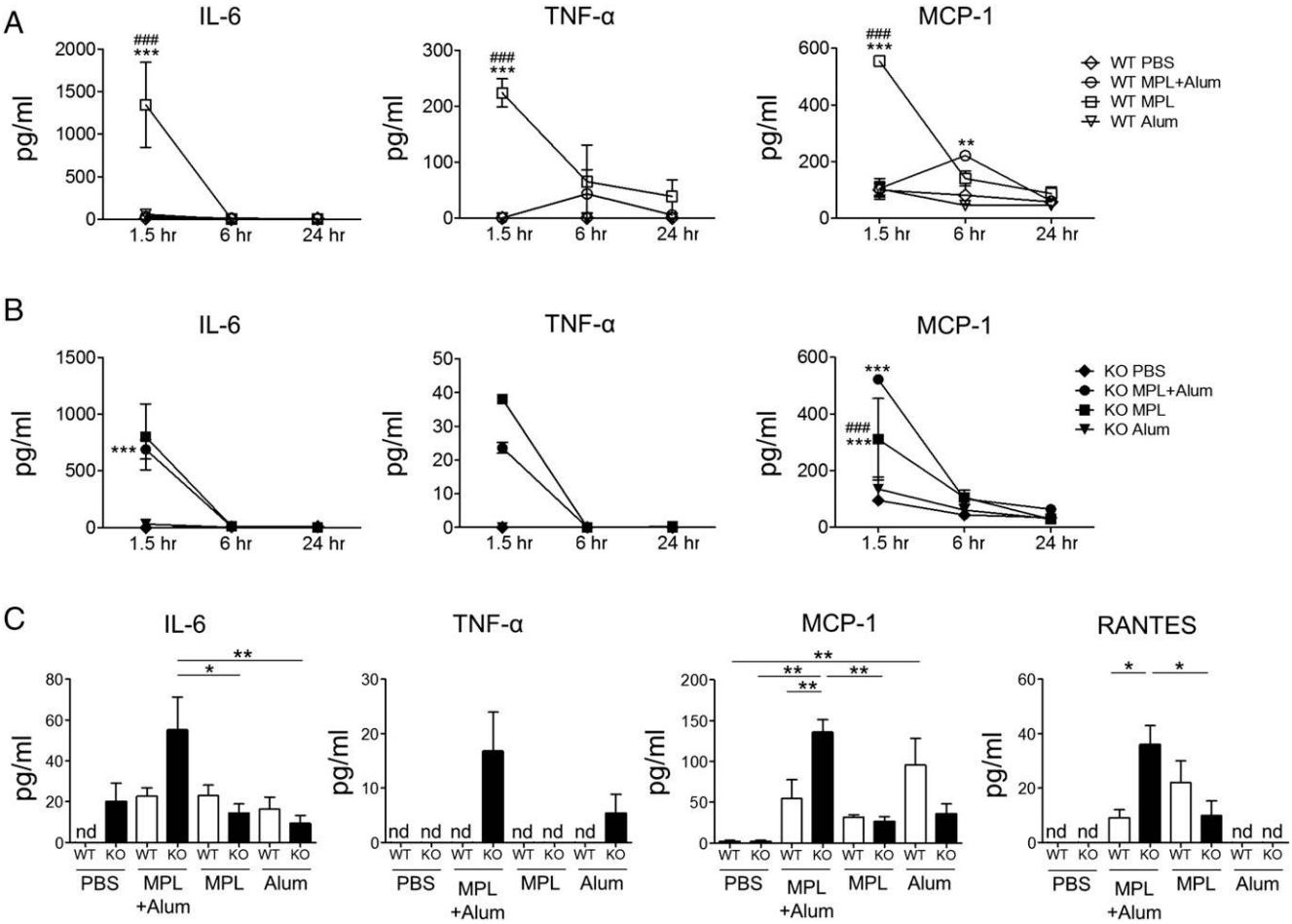

FIGURE 6. Levels of cytokines and chemokines in blood and peritoneal exudates after injection of adjuvants. WT and CD4KO mice ($n = 5$) were i.p. injected with 200 μl of PBS, MPL+Alum, MPL, or Alum. Kinetics of cytokines and chemokine levels in sera from adjuvant injected WT (**A**) and CD4KO (**B**) mice are shown. Statistical significance was calculated by two-way ANOVA and a Bonferroni posttest. $^{***}p < 0.001$ compared with PBS-treated group, $^{###}p < 0.001$ compared with MPL+Alum–treated group. (**C**) Cytokines and chemokines in peritoneal exudates at 24 h after peritoneal adjuvant injection. Statistical significance was calculated by one-way ANOVA and a Tukey multiple comparison test. $^{*}p < 0.05$, $^{**}p < 0.01$, $^{***}p < 0.001$ as indicated among the groups. KO, CD4KO mice; nd, not detected; WT, C57BL/6 WT mice.

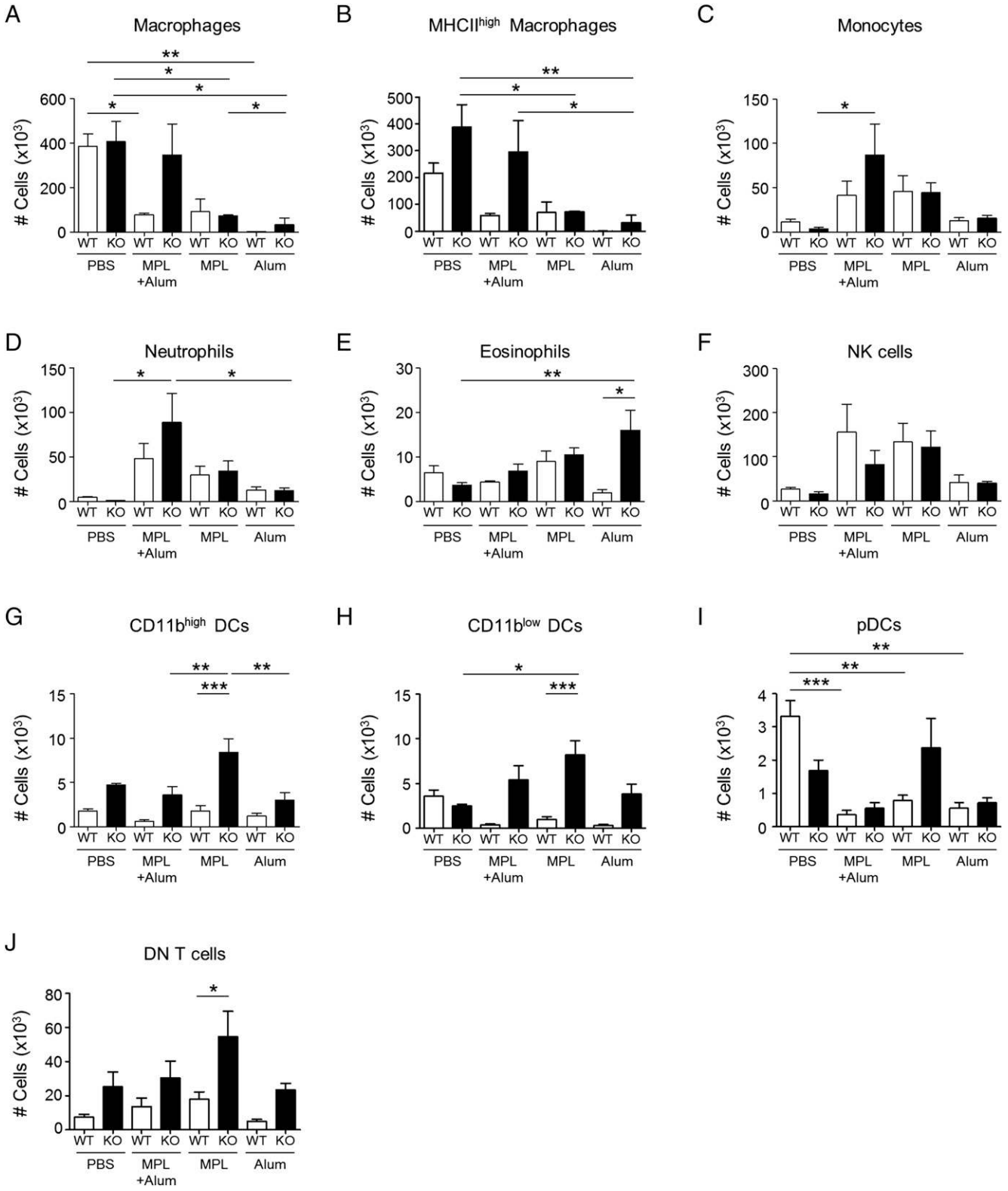

FIGURE 7. Recruitment of multiple immune cell phenotypes after adjuvant injection. (**A**–**J**) Cellularity of different phenotypic cells in peritoneal exudates from WT and CD4KO mice ($n = 5$). Cells in peritoneal exudates were collected at 24 h after adjuvant injection and their phenotypes and cellularity were determined. (A) Macrophages, $CD11b^+F4/80^+$. (B) $MHCII^{high}$ macrophages, $CD11b^+F4/80^+MHCII^{high}$. (C) Monocytes, $CD11b^+Ly6c^{high}F4/80^+$. (D) Neutrophils, $CD11b^+Ly6c^+F4/80^-$. (E) Eosinophils, $CD11b^+Siglec\text{-}F^+$. (F) $CD11b^{high}$ DCs, $CD11c^+CD11b^{high}MHCII^{high}$. (G) $CD11b^{low}$ DCs, $CD11c^+CD11b^{low}MHCII^{high}$. (H) pDCs, $CD11c^+B220^+MHCII^{high}$. (I) NK cells, $CD49b^+CD3^-$. (J) DN T cells, $CD3^+CD4^-CD8^-$. All data are shown as mean ± SEM. Statistical significance was calculated by one-way ANOVA and a Tukey multiple comparison test. $^*p < 0.05$, $^{**}p < 0.01$, $^{***}p < 0.001$ as indicated among the groups.

DCs (8%, Fig. 7H) in the peritoneal cavity, whereas CD4KO Alum maintained CD11b$^{low/high}$ DC populations compared with PBS controls (Fig. 7G, 7H). In contrast, WT-MPL+Alum mice had low levels (20–30%) of macrophages (CD11b$^+$F4/80$^+$, CD11b$^+$F4/80$^+$ MHCII^{high}, Fig. 7A, 7B), pDCs (11%, Fig. 7I), and CD11b^{low} DCs (10%, Fig. 7H) in the peritoneal cavity compared with those of PBS mock control mice (Fig. 7A, 7B, 7G–I). Differing from a profile in WT mice, MPL+Alum injection of CD4KO mice maintained the cellularity of macrophages (100%, Fig. 7A, 7B) and resulted in increasing CD11b^{low} DCs and CD11b^{high} DCs (Fig. 7G, 7H). Additionally, CD4KO MPL+Alum mice displayed significantly increased recruitment of neutrophils, monocytes, and NK cells by 76-, 23-, and 5-fold (Fig. 7C, 7D, 7F), respectively, which is a similar profile observed in WT-MPL+Alum mice. WT-MPL and CD4KO MPL mice showed a similar pattern of cellular changes in macrophages (reduced to 25%, Fig. 7A, 7B), monocytes (4-fold up, Fig. 6C), neutrophils (8-fold up, Fig. 7D), and NK cells (4-fold up, Fig. 7F). Uniquely, CD4KO MPL mice showed 2- to 4-fold increased levels of CD11b^{high} DCs, CD11b^{low} DCs, and pDCs compared with those in WT-MPL mice (Fig. 7G, 7H, 7I). KO-Alum mice recruited the highest level of eosinophils (4-fold) while reducing the levels of macrophages (<10%) and pDCs (<25%) in the peritoneal cavity compared with KO-PBS control mice (Fig. 7A, 7B, 7I). Additionally, CD4KO mice showed higher cellularity of the DN T cell (CD3$^+$CD4$^-$CD8$^-$) population, and MPL injection in both WT and CD4KO mice increased the DN T cells (2-fold compared with the PBS group) at the site of injection (Fig. 7J).

Overall, MPL+Alum KO mice maintained ~4- to 6-fold higher levels of MHCII^{high} macrophages and CD11b$^{high/low}$ DC populations compared with those in MPL+Alum WT mice. Also, 2- to 4-fold higher levels of CD11b$^{high/low}$ DC and DN T cell populations were observed in KO-MPL mice than in WT-MPL mice. These results suggest that differential cellularity of macrophages and DC populations together with DN T cells might be at least partially contributing to alternative B cell help in CD4KO mice.

MPL+Alum adjuvant combination attenuates the in vitro DC stimulatory effects by MPL

DCs are important cells to link between innate and adaptive immune responses. After 2-d cultures of DCs in the presence of adjuvants, cytokine levels in culture supernatants and activation marker expression on BMDCs were measured (Fig. 8A, 8B). MPL+Alum and MPL induced proinflammatory cytokine production by DCs, but Alum-treated DCs did not produce cytokines (Fig. 8A). MPL+Alum showed high levels of IL-6 and TNF-α but displayed a lower IL-12 cytokine level compared with the MPL alone adjuvant. In terms of DC activation markers, MPL showed significantly higher levels of CD40, CD80, and CD86 expression than did MPL+Alum on DCs (Fig. 8B). All adjuvants, that is, MPL+Alum, MPL, and Alum, increased MHCII^{high} DC populations (data not shown). These data indicate that Alum in MPL+Alum combination appears to attenuate stimulatory effects on DCs by MPL, a major player in in vitro activation of DCs.

To gain better understanding of in vivo adjuvant effects on reducing the cellularity of macrophages and DCs, we further tested in vitro cell death. Alum and MPL+Alum adjuvants were found to induce significant loss in cell viability after in vitro cultures of BM-derived primary cells (Fig. 8C).

To investigate a further possible mechanism of combination MPL+Alum adjuvant, we determined in vitro IgG production by B cells and proliferation of DN T cells after culture with or without adjuvant-pretreated BMDCs (Fig. 8D–F). MPL+Alum–pretreated BMDCs could support CD4KO mouse splenic B cells for IgG production in vitro, but splenic B cells with adjuvant only could not (Fig. 8D). Additionally, proliferation of DN T cells in CD4KO mouse splenocytes was stimulated by coculture with MPL+Alum–pretreated BMDCs, and MHCII mAb treatment suppressed its proliferation effects (Fig. 8E). Additionally, to determine cognate or noncognate help, we determined proliferation of DN T cells after incubation with MHCII$^+$ BMDCs stimulated with vaccine or nonvaccine Ags (Fig. 8F). Vaccine-treated BMDCs significantly increased the proliferation of DN T cells, but a different virus (A/Philippine H3N2) or OVA-treated BMDCs did not (Fig. 8F). These results provide evidence that MHCII$^+$ APCs contribute to stimulating Ag-specific DN T cells and providing alternative B cell help in a genetically CD4-deficient condition.

Discussion

Subunit vaccines provide a safe alternative to live-attenuated virus vaccines but have poor immunogenicity, requiring effective adjuvants to enhance the vaccine efficacy. Immune-competent mouse models are often highly responsive to experimental vaccines and adjuvants; however, they may not represent the efficacy expected in humans (24, 25). It is also thought that adjuvant effects are mediated by specific types of activated CD4$^+$ T cells that would be educated via MHCII-expressing APCs through multiple innate immune cellular interactions and the production of inflammatory cytokines resulting from adjuvant stimulation (7, 26–28). That is, vaccine adjuvants are important for modulating the types of CD4$^+$ T cells to induce the observed outcomes of adaptive immune responses in a conventional model. In contrast, the data in this study provide evidence that MPL+Alum adjuvant combination can mediate the induction of isotype-switched IgG Abs, conferring protective immunity in CD4KO mice comparable to those in WT mice even after 5 mo of vaccination. Therefore, this study suggests an alternative pathway and/or cells in providing help to the B cells for IgG production in CD4KO mice in the context of MPL+Alum– and MPL-adjuvanted influenza vaccination.

Alum adjuvants were unable to induce IgG Abs against split vaccine in CD4KO mice after prime. IgG1 Abs after boost immunization of CD4KO mice with Alum progressively waned to a further lower level after 3 mo (Table I). In contrast to Alum, MPL+Alum and MPL adjuvant effects were potent in WT and CD4KO mice even with prime only. The major difference between Alum and MPL+Alum is the induction of inflammatory cytokines, which was evident in vitro and in vivo. As expected, the results revealed that MPL- or MPL+Alum–activated BMDCs secrete IL-6 and TNF-α inflammatory cytokines, whereas Alum by itself did not. MPL+Alum did not directly stimulate CD4$^+$ T or B cells in vitro but was shown to directly activate DCs in vitro primarily due to MPL, leading to the induction of Ag-specific T cells in vivo (29). Therefore, the microenvironment creating inflammatory cytokines by MPL+Alum and MPL is likely to play a major role in priming IgG isotype–switched B cell response in CD4KO mice. Previous studies demonstrated that mice lacking CD40 or CD4$^+$ T cells during sublethal primary infection induced only short-lived IgG Abs waning within 60 d and no Ab-secreting plasma cells (21, 22). Therefore, the results of long-lived IgG Ab responses mediated by MPL+Alum and MPL adjuvant in CD4KO mice are particularly notable.

The mechanisms of adjuvant effects on enhancing vaccine efficacy remain poorly understood, particularly in a CD4-deficient condition, although CD4-independent activation of CD8$^+$ T cells and B cells has been reported. DN αβ T cells were shown to play a role in generating CD4-independent isotype-switched IgG Abs using CD4KO and TCRβ KO mouse models (30). Another study

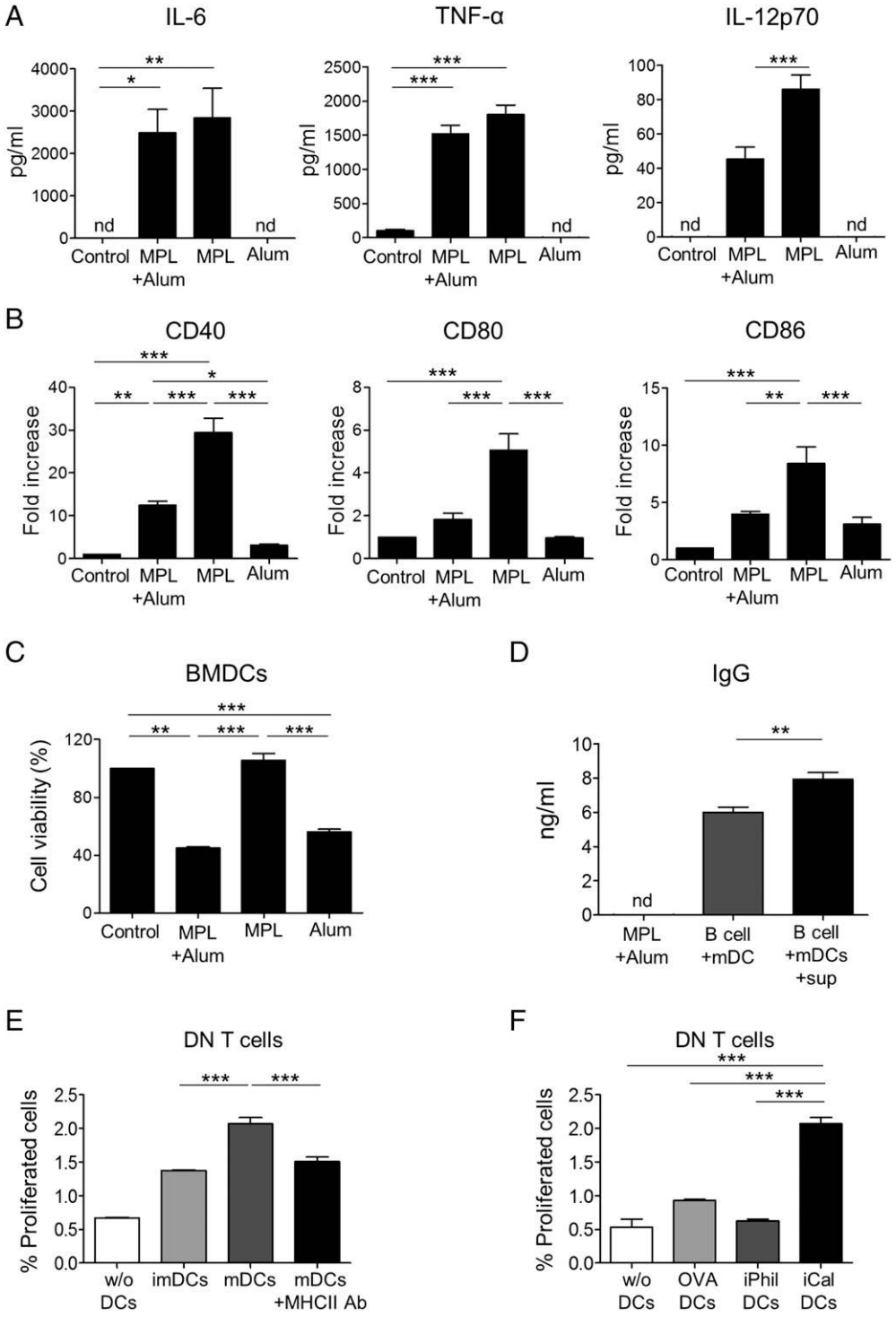

FIGURE 8. In vitro effects of adjuvants on DC activation or cell death. (**A**) Proinflammatory cytokine production of BMDCs after adjuvant treatment. (**B**) Activation marker expression on adjuvant-treated BMDCs. Fold increase of marker expression was determined by mean fluorescence index of each group compared with that of the control group. BMDCs were generated from BM cells of WT mice. BMDCs were cultured with media (control) or adjuvants for 48 h. (**C**) Cell viability of BMDCs treated with MPL+Alum, MPL, or Alum. Cell viability was determined by an MTT assay after 2 d of culture with adjuvants. (**D**) In vitro Ab production by adjuvant-treated BMDCs. Spleen cells containing naive B cells were harvested from naive CD4KO mice and cultured with MPL+Alum, MPL+Alum–pretreated mDCs, or mDC plus mDC culture supernatants (sup, a source of cytokines). The mDCs were prepared by pretreating with adjuvants for 2 d. After 7 d of culture, total IgG levels in culture supernatants were determined by ELISA. (**E**) Percentages of proliferated DN ($CD4^-CD8^-$ in $CD3^+$ T cells) T cells after 5 d coculture with or without BMDCs. imDCs, DN T cells cultured with untreated control BMDCs; mDCs, DN T cells cultured with MPL+Alum–pretreated BMDCs; mDCs+MHCII Ab, DN T cells cultured with MPL+Alum and anti-mouse MHCII (clone M5/114.15.2) Ab (1 μg/ml)–pretreated BMDCs; w/o DCs, CD4KO mouse splenocytes containing DN T cells were cultured without BMDCs, and proliferation of CFSE-labeled DN T cells was analyzed by flow cytometry. (**F**) Percentages of proliferated DN ($CD4^-CD8^-$ in $CD3^+$ T cells) T cells after 5 d coculture with different Ag-treated BMDCs. iCal DCs, DN T cells were cultured with inactivated A/California H1N1 virus vaccine strain pretreated BMDCs; iPhil DCs, DN T cells were cultured with inactivated A/Philippine H3N2 virus–pretreated BMDCs; OVA DCs, DN T cells were cultured with OVA-pretreated BMDCs; w/o DCs, CD4KO mouse splenocytes containing DN T cells were cultured without BMDCs. All data are shown as mean ± SEM. Statistical significance was calculated by one-way ANOVA and a Tukey multiple comparison test. $*p < 0.05$, $**p < 0.01$, $***p < 0.001$ as indicated among the groups. nd, not detected.

demonstrated that both B7-1 (CD80) and B7-2 (CD86) costimulatory molecules on DCs were required for IgG1 and IgG2a responses (31). The TNF-α pathway was important for activating cytotoxic effector CD8$^+$ T cells in the absence of CD4 T cells (32). This study provides evidence that a CD4 genetic defect led to developing other compensatory immune components even in a mock (PBS) treatment condition. PBS treatment of CD4KO mice showed higher levels of MHCII^{high} macrophages, CD11b^{high} DCs, DN T cells, and a lower level of pDCs compared with those in WT mice. Upon treatment with combination MPL+Alum adjuvant, CD4KO mice further increased cellularity of MHCII^{high} macrophages and CD11b^{high} and CD11b^{low} DCs compared with those in WT mice, in addition to comparable increases in monocytes, neutrophils, NK cells, and eosinophils. These cellular increases at the site of injection appeared to be correlated with high levels of cytokines (IL-6, TNF-α) and chemokines (MCP-1, RANTES) upon treatment of CD4KO mice with combination MPL+Alum adjuvant. Meanwhile, MPL-treated CD4KO mice showed increased levels in DC populations (CD11b^{high}, CD11b^{low} DCs, pDCs) and DN T cells compared with those in MPL-treated WT mice. We also observed further increased levels of DCs, but not macrophages, compared with those in MPL+Alum–treated CD4KO mice. Thus, it is possible that cellular components contributing to alternative B cell help in CD4KO mice are likely to be different between MPL (mostly various DC subsets, DN T cells) and combination MPL+Alum (mostly macrophages, minimally CD11b^{low} DCs) adjuvants.

To gain further insight into possible roles of these compensatory immune components in providing alternative B cell help in CD4KO mice, we determined IgG responses in acutely CD4-depleted WT mice. We observed lower levels of IgG responses in CD4-depleted WT mice with MPL and MPL+Alum compared with those in CD4KO mice with the same adjuvanted vaccination. Thus, it is possible that compensatory immune components, including MHCII^{high} macrophages, DC populations, and DN T cells, developed in CD4KO mice are contributing to overcoming defects in CD4 help to B cells for the generation of isotype-switched Abs by MPL and combination MPL+Alum vaccination. In line with these results, MHCII KO mice with MPL+Alum adjuvant vaccination were found to induce lower levels of IgG responses by 32-fold than those in CD4KO mice with the same adjuvant vaccination (Table I). Additionally, MPL+Alum–activated BMDCs might have the capability to stimulate naive splenic B cells to secrete IgG Abs in vitro. Because efficient naive CD4$^+$ T cell priming does not require B cells expressing MHCII (33), MHCII-expressing APCs such as DCs and macrophages significantly contribute to the generation of isotype-switched IgG Abs, probably via an alternative pathway different from conventional CD4$^+$ T cell help.

Adjuvant roles of Alum and MPL in MPL+Alum combination are yet to be fully understood. Differences in serum IgG Ab levels between MPL+Alum and MPL appeared to be greater at a later time point of 3 mo boost in CD4KO mice (Table I), which are further supported by ASC responses in spleens. Alum in AS04 (MPL+Alum) appeared to have a property of attenuating innate immune-stimulating activities by MPL in vitro and in vivo. MPL was found to highly upregulate the expression of costimulatory molecules (CD40, CD80, and CD86) on BMDCs, which can provide alternative B cell help to produce isotype-switched Abs (34). Meanwhile, MPL+Alum appeared to moderately suppress the stimulatory effects of MPL on upregulating costimulatory molecules and IL-12 cytokine production during BMDC in vitro cultures. Attenuating acute induction of inflammatory cytokines would improve the safety for AS04 adjuvant–formulated human vaccination.

Adjuvant-induced cell death has been known to be a mechanism of adjuvanticity for more than a decade (35), although cell death is often considered an undesirable side effect. TNF family cytokines are classic inducers of programmed necrosis via receptor-interacting protein kinases, which promotes inflammation (36). Alum was demonstrated to induce uric acid by causing sterile cell death (37). Also, there is a well-known link between TLR activation and cell death leading to proapoptotic activities (38). We found that in vitro cultures of BMDCs with Alum or MPL+Alum resulted in cell death. In in vivo studies, WT mice with Alum, MPL+Alum, or MPL injection resulted in a significant loss of macrophages, CD11b^{low} DCs, and pDCs in the peritoneal cavity. CD4KO mice with Alum or MPL injection exhibited a significant loss in macrophages in the peritoneal cavity whereas MPL+Alum retained up to 80% of macrophages. Thus, MPL+Alum adjuvant combination might be contributing to protect macrophages from a severe cellular loss in the in vivo injection site in WT mice compared with Alum, and more prominently in CD4KO mice compared with Alum and MPL.

In summary, MPL+Alum showed effective adjuvant effects on inducing IgG isotype-switched Abs and conferring protective immunity in CD4KO mice, which was more effective compared with those in WT mice with influenza vaccine only or Alum-adjuvanted vaccination. MPL+Alum showed moderate levels of cytokines (IL-6, TNF-α) and chemokines (MCP-1, RANTES) in the peritoneal cavity at 24 h after injection of CD4KO mice. MPL+Alum appears to have differential effects on generating a local inflammatory microenvironment, maintaining macrophages, and attenuating acute inflammation compared with those of MPL and Alum. MHCII-expressing cellular components, DN T cells, and soluble cytokines and chemokines at the site of injection are likely to be the major contributing factors in providing alternative help to B cells for inducing IgG Ab responses in the context of MPL+Alum–adjuvanted influenza vaccination of CD4KO mice.

Disclosures

The authors have no financial conflicts of interest.

References

1. Young, B. E., S. P. Sadarangani, and Y. S. Leo. 2015. The avian influenza vaccine Emerflu. Why did it fail? *Expert Rev. Vaccines* 14: 1125–1134.
2. Kim, H. W., J. G. Canchola, C. D. Brandt, G. Pyles, R. M. Chanock, K. Jensen, and R. H. Parrott. 1969. Respiratory syncytial virus disease in infants despite prior administration of antigenic inactivated vaccine. *Am. J. Epidemiol.* 89: 422–434.
3. Garçon, N., P. Chomez, and M. Van Mechelen. 2007. GlaxoSmithKline adjuvant systems in vaccines: concepts, achievements and perspectives. *Expert Rev. Vaccines* 6: 723–739.
4. Paavonen, J., D. Jenkins, F. X. Bosch, P. Naud, J. Salmerón, C. M. Wheeler, S. N. Chow, D. L. Apter, H. C. Kitchener, X. Castellsague, et al; HPV PATRICIA study group. 2007. Efficacy of a prophylactic adjuvanted bivalent L1 virus-like-particle vaccine against infection with human papillomavirus types 16 and 18 in young women: an interim analysis of a phase III double-blind, randomised controlled trial. *Lancet* 369: 2161–2170.
5. Kundi, M. 2007. New hepatitis B vaccine formulated with an improved adjuvant system. *Expert Rev. Vaccines* 6: 133–140.
6. Coffman, R. L., A. Sher, and R. A. Seder. 2010. Vaccine adjuvants: putting innate immunity to work. *Immunity* 33: 492–503.
7. McAleer, J. P., and A. T. Vella. 2010. Educating CD4 T cells with vaccine adjuvants: lessons from lipopolysaccharide. *Trends Immunol.* 31: 429–435.
8. Sangster, M. Y., J. M. Riberdy, M. Gonzalez, D. J. Topham, N. Baumgarth, and P. C. Doherty. 2003. An early CD4+ T cell–dependent immunoglobulin A response to influenza infection in the absence of key cognate T–B interactions. *J. Exp. Med.* 198: 1011–1021.
9. Burns, W., L. C. Billups, and A. L. Notkins. 1975. Thymus dependence of viral antigens. *Nature* 256: 654–656.
10. Iwasaki, T., and T. Nozima. 1977. Defense mechanisms against primary influenza virus infection in mice. I. The roles of interferon and neutralizing antibodies and thymus dependence of interferon and antibody production. *J. Immunol.* 118: 256–263.
11. Scherle, P. A., and W. Gerhard. 1986. Functional analysis of influenza-specific helper T cell clones in vivo. T cells specific for internal viral proteins provide

cognate help for B cell responses to hemagglutinin. *J. Exp. Med.* 164: 1114–1128.
12. Pulendran, B., and R. Ahmed. 2006. Translating innate immunity into immunological memory: implications for vaccine development. *Cell* 124: 849–863.
13. Kawai, T., and S. Akira. 2007. TLR signaling. *Semin. Immunol.* 19: 24–32.
14. Pulendran, B. 2004. Modulating vaccine responses with dendritic cells and Toll-like receptors. *Immunol. Rev.* 199: 227–250.
15. Quan, F. S., C. Huang, R. W. Compans, and S. M. Kang. 2007. Virus-like particle vaccine induces protective immunity against homologous and heterologous strains of influenza virus. *J. Virol.* 81: 3514–3524.
16. O, E., Y. T. Lee, E. J. Ko, K. H. Kim, Y. N. Lee, J. M. Song, Y. M. Kwon, M. C. Kim, D. R. Perez, and S. M. Kang. 2014. Roles of major histocompatibility complex class II in inducing protective immune responses to influenza vaccination. *J. Virol.* 88: 7764–7775.
17. Kwon, Y. M., H. S. Hwang, J. S. Lee, E. J. Ko, S. E. Yoo, M. C. Kim, Y. N. Lee, K. H. Kim, J. M. Song, S. Lee, et al. 2014. Maternal antibodies by passive immunization with formalin inactivated respiratory syncytial virus confer protection without vaccine-enhanced disease. *Antiviral Res.* 104: 1–6.
18. Hwang, H. S., Y. M. Kwon, J. S. Lee, S. E. Yoo, Y. N. Lee, E. J. Ko, M. C. Kim, M. K. Cho, Y. T. Lee, Y. J. Jung, et al. 2014. Co-immunization with virus-like particle and DNA vaccines induces protection against respiratory syncytial virus infection and bronchiolitis. *Antiviral Res.* 110: 115–123.
19. Lee, Y. N., M. C. Kim, Y. T. Lee, H. S. Hwang, M. K. Cho, J. S. Lee, E. J. Ko, Y. M. Kwon, and S. M. Kang. 2014. AS04-adjuvanted virus-like particles containing multiple M2 extracellular domains of influenza virus confer improved protection. *Vaccine* 32: 4578–4585.
20. Song, J. M., J. Hossain, D. G. Yoo, A. S. Lipatov, C. T. Davis, F. S. Quan, L. M. Chen, R. J. Hogan, R. O. Donis, R. W. Compans, and S. M. Kang. 2010. Protective immunity against H5N1 influenza virus by a single dose vaccination with virus-like particles. *Virology* 405: 165–175.
21. Lee, B. O., J. Rangel-Moreno, J. E. Moyron-Quiroz, L. Hartson, M. Makris, F. Sprague, F. E. Lund, and T. D. Randall. 2005. CD4 T cell-independent antibody response promotes resolution of primary influenza infection and helps to prevent reinfection. *J. Immunol.* 175: 5827–5838.
22. Tonti, E., M. Fedeli, A. Napolitano, M. Iannacone, U. H. von Andrian, L. G. Guidotti, S. Abrignani, G. Casorati, and P. Dellabona. 2012. Follicular helper NKT cells induce limited B cell responses and germinal center formation in the absence of $CD4^+$ T cell help. *J. Immunol.* 188: 3217–3222.
23. Grusby, M. J., R. S. Johnson, V. E. Papaioannou, and L. H. Glimcher. 1991. Depletion of $CD4^+$ T cells in major histocompatibility complex class II-deficient mice. *Science* 253: 1417–1420.
24. Mestas, J., and C. C. Hughes. 2004. Of mice and not men: differences between mouse and human immunology. *J. Immunol.* 172: 2731–2738.
25. Dormitzer, P. R., G. Galli, F. Castellino, H. Golding, S. Khurana, G. Del Giudice, and R. Rappuoli. 2011. Influenza vaccine immunology. *Immunol. Rev.* 239: 167–177.
26. O'Hagan, D. T., G. S. Ott, E. De Gregorio, and A. Seubert. 2012. The mechanism of action of MF59—an innately attractive adjuvant formulation. *Vaccine* 30: 4341–4348.
27. McKee, A. S., M. K. MacLeod, J. W. Kappler, and P. Marrack. 2010. Immune mechanisms of protection: can adjuvants rise to the challenge? *BMC Biol.* 8: 37.
28. McAleer, J. P., D. J. Zammit, L. Lefrançois, R. J. Rossi, and A. T. Vella. 2007. The lipopolysaccharide adjuvant effect on T cells relies on nonoverlapping contributions from the MyD88 pathway and $CD11c^+$ cells. *J. Immunol.* 179: 6524–6535.
29. Didierlaurent, A. M., S. Morel, L. Lockman, S. L. Giannini, M. Bisteau, H. Carlsen, A. Kielland, O. Vosters, N. Vanderheyde, F. Schiavetti, et al. 2009. AS04, an aluminum salt- and TLR4 agonist-based adjuvant system, induces a transient localized innate immune response leading to enhanced adaptive immunity. *J. Immunol.* 183: 6186–6197.
30. Sha, Z., and R. W. Compans. 2000. Induction of $CD4^+$ T-cell-independent immunoglobulin responses by inactivated influenza virus. *J. Virol.* 74: 4999–5005.
31. Rauschmayr-Kopp, T., I. R. Williams, F. Borriello, A. H. Sharpe, and T. S. Kupper. 1998. Distinct roles for B7 costimulation in contact hypersensitivity and humoral immune responses to epicutaneous antigen. *Eur. J. Immunol.* 28: 4221–4227.
32. Zimmerer, J. M., P. H. Horne, L. A. Fiessinger, M. G. Fisher, T. A. Pham, S. L. Saklayen, and G. L. Bumgardner. 2012. Cytotoxic effector function of CD4-independent, $CD8^+$ T cells is mediated by TNF-α/TNFR. *Transplantation* 94: 1103–1110.
33. Williams, G. S., A. Oxenius, H. Hengartner, C. Benoist, and D. Mathis. 1998. $CD4^+$ T cell responses in mice lacking MHC class II molecules specifically on B cells. *Eur. J. Immunol.* 28: 3763–3772.
34. Rau, F. C., J. Dieter, Z. Luo, S. O. Priest, and N. Baumgarth. 2009. B7-1/2 (CD80/CD86) direct signaling to B cells enhances IgG secretion. *J. Immunol.* 183: 7661–7671.
35. Ferguson, T. A., J. Choi, and D. R. Green. 2011. Armed response: how dying cells influence T-cell functions. *Immunol. Rev.* 241: 77–88.
36. Moriwaki, K., and F. K. Chan. 2013. RIP3: a molecular switch for necrosis and inflammation. *Genes Dev.* 27: 1640–1649.
37. Kono, H., C. J. Chen, F. Ontiveros, and K. L. Rock. 2010. Uric acid promotes an acute inflammatory response to sterile cell death in mice. *J. Clin. Invest.* 120: 1939–1949.
38. Schön, M. P., B. G. Wienrich, C. Drewniok, A. B. Bong, J. Eberle, C. C. Geilen, H. Gollnick, and M. Schön. 2004. Death receptor-independent apoptosis in malignant melanoma induced by the small-molecule immune response modifier imiquimod. *J. Invest. Dermatol.* 122: 1266–1276.